

Semiquantitative Parameters in PSMA-Targeted PET Imaging with [¹⁸F]DCFPyL: Impact of Tumor Burden on Normal Organ Uptake

Rudolf A. Werner,^{1,2,3,4} Ralph A. Bundschuh,⁵ Lena Bundschuh,⁵ Constantin Lapa,² Yafu Yin,^{1,6,7} Mehrbod S. Javadi,¹ Andreas K. Buck,^{2,3} Takahiro Higuchi,^{2,3,8} Kenneth J. Pienta,⁹ Martin G. Pomper,^{1,9} Martin A. Lodge,¹ Michael A. Gorin,^{1,9} Steven P. Rowe^{1,9,10}

¹The Russell H. Morgan Department of Radiology and Radiological Science, Johns Hopkins University School of Medicine, Baltimore, MD, USA

²Department of Nuclear Medicine, University Hospital Würzburg, Würzburg, Germany

³Comprehensive Heart Failure Center, University Hospital Würzburg, Würzburg, Germany

⁴Department of Nuclear Medicine, Hannover Medical School, Hannover, Germany

⁵Department of Nuclear Medicine, University Medical Center Bonn, Bonn, Germany

⁶Department of Nuclear Medicine, The First Hospital of China Medical University, Shenyang, China

⁷Department of Nuclear Medicine, Xinhua Hospital, Shanghai Jiao Tong University School of Medicine, Shanghai, China

⁸Dentistry and Pharmaceutical Sciences, Okayama University Graduate School of Medicine, Okayama, Japan

⁹The James Buchanan Brady Urological Institute and Department of Urology, Johns Hopkins University School of Medicine, Baltimore, MD, USA

¹⁰Division of Nuclear Medicine and Molecular Imaging, The Russell H. Morgan Department of Radiology and Radiological Science, Johns Hopkins University School of Medicine, 601 N. Caroline St., Baltimore, MD, 21287, USA

Abstract

Purpose: In this study, we aimed to quantitatively investigate the biodistribution of [¹⁸F]DCFPyL in patients with prostate cancer (PCa) and to determine whether uptake in normal organs correlates with an increase in tumor burden.

Procedures: Fifty patients who had been imaged with [¹⁸F]DCFPyL positron emission tomography/computed tomography (PET/CT) were retrospectively included in this study. Forty of 50 (80 %) demonstrated radiotracer uptake on [¹⁸F]DCFPyL PET/CT compatible with sites of PCa. Volumes of interests (VOIs) were set on normal organs (lacrimal glands, parotid glands, submandibular glands, liver, spleen, and kidneys) and on tumor lesions. Mean standardized uptake values corrected to lean body mass (SUL_{mean}) and mean standardized uptake values corrected to body weight (SUV_{mean}) for normal organs were assessed. For the entire tumor burden, SUL_{mean/max}, SUV_{mean}, tumor volume (TV), and the total activity in the VOI were obtained using tumor segmentation. A Spearman's rank correlation coefficient was used to investigate correlations between normal organ uptake and tumor burden.

Results: There was no significant correlation between TV with the vast majority of the investigated organs (lacrimal glands, parotid glands, submandibular glands, spleen, and liver).

Only the kidney showed significant correlation: With an isocontour threshold at 50 %, left kidney uptake parameters correlated significantly with TV (SUV_{mean} , $\rho = -0.214$ and SUL_{mean} , $\rho = -0.176$, $p < 0.05$, respectively).

Conclusions: Only a minimal sink effect with high tumor burden in patients imaged with [^{18}F]DCFPyL was observed. Other factors, such as a high intra-patient variability of normal organ uptake, may be a much more important consideration for personalized dosimetry with PSMA-targeted therapeutic agents structurally related to [^{18}F]DCFPyL than the tumor burden.

Key words: Prostate-specific membrane antigen, Positron emission tomography, Biodistribution, [^{18}F]DCFPyL, PSMA

Introduction

Novel imaging agents targeting prostate-specific membrane antigen (PSMA) have demonstrated excellent diagnostic accuracy for visualizing sites of prostate cancer (PCa) [1–3]. Although Ga-68-labeled radiotracers targeting PSMA have been more commonly used, novel F-18-labeled radiotracers, such as [^{18}F]DCFPyL, are increasingly utilized and there have been suggestions of superior imaging characteristics relative to Ga-68-labeled compounds [4–7]. In a similar vein to the theranostics twins [^{68}Ga]/[^{177}Lu] 1,4,7,10-tetraazacyclododecane-N,N',N'',N'''-tetraacetic acid-d-Phe(1)-Tyr(3)-octreotide/-octreotate (DOTATOC/-TATE) used for the diagnosis and treatment of neuroendocrine tumors (NET), the theranostic concept has been extended to PCa with the introduction of Lu-177-labeled PSMA-targeted compounds [8]. As a result, it is imperative to understand the fundamental factors that can affect PSMA-targeted radiotracer biodistribution and how those factors might affect both diagnostic accuracy and therapy planning. Indeed, the biodistribution of PSMA-targeted positron emission tomography (PET) imaging involves complex interplay of varying factors, such as renal excretion, physiologic uptake and retention in normal organs, normal variant uptake in benign lesions, and uptake in PCa tumor lesions.

As reported previously, radiotracers may be prone to the impact of tumor uptake on normal organ biodistribution [9–11]. For example, Beauregard et al. reported declines in [^{68}Ga]DOTATATE uptake in normal organs in patients with increasing NET burden and suggested to adapt the therapeutic activity with a Lu-177-labeled compound to the tumor load [11]. In contrast, our group recently reported that there was no such tumor sink effect using the lower affinity somatostatin receptor imaging probe [^{68}Ga]DOTATOC [12]. In regard to PSMA-targeted radiotracers in patients with PCa, Gärtner et al. reported on a decline of [^{68}Ga]PSMA-11 uptake in kidneys in patients with higher tumor burden [13].

Given the current trend towards increased use of F-18-labeled PSMA-ligands [4, 5], we sought to investigate factors that may have an impact on semiquantitative parameters in PSMA-targeted PET imaging with [^{18}F]DCFPyL: First, in a companion study, we aimed to investigate the inter-patient and intra-patient variability of semiquantitative parameters in the most relevant normal organs

[14], while in the present paper, the biodistribution of [^{18}F]DCFPyL in PCa patients with different tumor burdens was quantitatively investigated. As this may have implications for a theranostic approach using Lu-177-labeled ligands structurally related to [^{18}F]DCFPyL, we aimed to clarify whether uptake in normal organs may correlate with an increase in tumor burden.

Methods

Patient Population

In total, 50 patients with histologically proven PCa who had undergone [^{18}F]DCFPyL PET/computed tomography (CT) imaging were included in this evaluation. All patients were originally imaged as part of an institutional review board-approved protocol (ClinicalTrials.gov identifier NCT02825875) and signed written informed consent prior to imaging. The current study is a *post hoc* analysis of the referenced prospective trial. [^{18}F]DCFPyL was used under an Investigational New Drug application from the US Food and Drug Administration (IND 121064). A detailed description of this patient cohort can be found in Table 1 [15].

Table 1. Detailed patients' characteristics

Age (median \pm SD, in years)		65 \pm 8
Height (m)		1.78 \pm 0.06
Weight (kg)		88 \pm 15
Indication for Scan	Staging	24/50 (48 %)
	Biochemical recurrence	9/50 (18 %)
	Biochemical persistence after primary surgery	6/50 (12 %)
	Primary diagnosis	5/50 (10 %)
	Potential withdrawal of androgen deprivation therapy	3/50 (6 %)
	Other	3/50 (6 %)
PSA level (ng/ml)	Overall (median (range))	3.2 (0.02–48)
Prior therapies	In total	41/50 (82 %)
	Surgery	29/41 (70.7 %)
	Hormonal therapy	21/41 (51.2 %)
	RTx	18/41 (43.9 %)
	CTx	6/41 (14.6 %)

Modified from Werner et al. [15], © by the Society of Nuclear Medicine and Molecular Imaging
SD standard deviation, CTx chemotherapy, PSA prostate-specific antigen, RTx radiation therapy

Imaging Procedure

As per standard practice at our institution, patients were asked to be *nil per os* (with the exception of water and medications) for a minimum of 4 h prior to radiotracer injection. [¹⁸F]DCFPyL was synthesized under current good manufacturing practice conditions as has been previously described [16]. Integrated PET/CT using either a Discovery RX 64-slice PET/CT (General Electric, Waukesha, Wisconsin, USA) or a Biograph mCT 128-slice PET/CT (Siemens, Erlangen, Germany) was performed in all patients. The PET scanners were operated in 3D emission mode with CT attenuation correction. [¹⁸F]DCFPyL ≤ 333 MBq (≤ 9 mCi) was administered through a peripheral intravenous catheter and after an uptake time of approximately 60 min, acquisitions from the mid-thigh to the vertex of the skull were conducted, covering six to eight bed positions. The patients were in the supine position. For further details, please refer to [17].

Imaging Analysis

PET images were analyzed using XD3 software (Mirada Medical, Oxford, UK). PET, CT, and hybrid PET/CT imaging overlays were assessed in the axial, sagittal, and coronal planes in all 50 patients. Lesions were identified as abnormal foci of radiotracer uptake above background and in expected patterns for PCa spread [18, 19]. Lesions were selected by a single reader experienced in the interpretation of PSMA-targeted PET (MSJ) and verified by a second experienced reader (SPR).

The normal biodistribution of [¹⁸F]DCFPyL includes uptake in the lacrimal glands, parotid glands, and submandibular glands, as well as in the liver, spleen, kidneys, and bowel (predominantly proximal small bowel) [18, 19]. For the lacrimal glands, major salivary glands, liver, spleen, and kidneys, volume of interests (VOIs) were manually set covering the entire organ volume using the best visual approximation of the organ edge on the PET images using previously described methodology [20]. Moreover, as described in [12], the entire volume of all [¹⁸F]DCFPyL-avid tumor lesions (*i.e.*, tumor burden) was manually segmented using the same procedure. The CT images were not used as a primary guide for the segmentation of the VOIs but were available as a reference to improve VOI placement in regions of complex anatomy or high background radiotracer uptake, as necessary [20].

For normal organs, the following parameters were recorded: mean standardized uptake value corrected to lean body mass (SUL_{mean}) and mean standardized uptake value corrected to body weight (SUV_{mean}) [17, 20]. For the entire tumor burden, the following parameters were assessed: SUL_{mean} , the maximum standardized uptake value corrected to lean body mass (SUL_{max}), SUV_{mean} , tumor volume (TV), and the fractional tumor activity (FTA) in the VOI. The latter parameter is well-

established in the literature and has also been referred to as tumor lesion (TL)-PSMA [21, 22]. FTA was calculated as follows: $[TV \times SUV_{\text{mean}}]$. An isocontour threshold of 50 % of the SUV_{max} was determined between the background and the maximal pixel value of the VOI.

Statistical Analysis

Percentiles are reported to describe the distribution of the parameters. Additionally, mean \pm standard deviation is provided for parameters with a normal distribution as determined with the Shapiro-Wilk test. Spearman's rank correlation coefficient (Spearman's Rho, ρ) was used to assess the correlations between parameters. Statistical analysis was performed using MedCalc Statistical Software (version 18.2.1, MedCalc Software bvba, Ostend, Belgium). The statistical significance level was set at $p < 0.05$.

Results

Patient Population

The median age of the cohort was 65 ± 8 years (range, 44–77 years). The majority of the subjects were of white race (38/50, 76.0 %). The clinical indications for performing an [¹⁸F]DCFPyL PET/CT were as follows: staging in 24/50 (48.0 %), biochemical recurrence in 9/50 (18.0 %), biochemical persistence after surgery in 6/50 (12.0 %), primary diagnostic assessment in 5/50 (10.0 %), potential withdrawal of hormonal therapy in 3/50 (6.0 %), and other reasons in 3/50 (6.0 %). The median prostate-specific antigen level was 3.2 ng/ml (0.02–48), and 41/50 (82.0 %) patients had therapy prior to [¹⁸F]DCFPyL PET/CT: surgery in 29/41 (70.7 %), hormonal therapy in 21/41 (51.2 %), radiotherapy in 18/41 (43.9 %), and chemotherapy in 6/41 (14.6 %). Additional details of the study population are provided in Table 1.

Quantitative Assessment

In those patients with discernible tumor radiotracer uptake ($n = 40$), a total of 243 VOIs were placed (median, 3 per patient; range, 1–78) to generate data for tumor burden. One hundred thirty-seven of 243 (56.4 %) of the VOIs were set on bone lesions, 87/243 (35.8 %) were placed on lymph nodes (LNs), 13/243 (5.3 %) were placed on non-LN soft tissue sites, 5/243 (2.1 %) were placed on lung lesions, and 1 (0.4 %) VOI was placed on a liver lesion. For normal organs, the following values (median) were recorded: For SUL_{mean} : left lacrimal gland 3.6 and right lacrimal gland 3.7; left parotid gland 6.0 and right parotid gland 6.3; left submandibular gland 5.8 and right submandibular gland 5.9; liver 3.7; spleen 2.6; left kidney 16.6 and right kidney 17.3. For SUV_{mean} : left lacrimal gland 4.9 and right lacrimal gland 5.1; left parotid gland 8.1 and right parotid gland 8.2; left submandibular gland 7.9 and right submandibular gland 8.0;

liver 5.0; spleen 3.7; left kidney 22.8 and right kidney 23.4. For tumor burden, the median values for SUL_{mean} , SUL_{max} , SUV_{mean} , TV , and FTA are displayed in Table 2.

Correlative Analysis Between Tumor Burden vs. Normal Organ Uptake and Inter-Organ Correlations

There was no significant correlation between TV with the vast majority of the investigated organs (lacrimal glands, parotid glands, submandibular glands, spleen and liver). Only the kidney showed significant correlations with tumor burden parameters: SUV_{mean} and SUL_{mean} of the left kidney correlated with TV using an intensity threshold of 50 % (Table 3: SUV_{mean} , $\rho = -0.214$ and SUL_{mean} , $\rho = -0.176$, $p < 0.05$, respectively; Fig. 1a, b). Table 3 displays Spearman's Rho and Fig. 1 demonstrates correlative plots for the relations between normal organs and tumor burden. Figure 2 displays three patients with different tumor burden: (a) low, (b) intermediate, and (c) high and reflects visually no significant decrease in normal organ uptake with increasing tumor burden.

Discussion

PSMA-targeted radiotracers such as $[^{18}F]DCFPyL$ have demonstrated significantly improved imaging characteristics for identifying sites of PCa relative to conventional imaging

[6, 23]. The widespread use of these agents and their ability to select patients for PSMA-targeted therapies necessitate a complete understanding of the parameters that dictate normal organ uptake. As such, in this manuscript, we aimed to continue an exploration of the factors that may influence semiquantification of $[^{18}F]DCFPyL$ studies. Thus, in a companion paper, the impact of intra-/inter-patient variability on relevant normal organs was assessed [14], while in the present study, we investigated the impact of tumor burden on normal organ uptake.

First and foremost, the majority of the herein investigated organs (lacrimal glands, parotid glands, submandibular glands, spleen, and liver) did not show significant correlations with any of the parameters assessing the tumor burden. Only a moderate significant inverse correlation for the kidneys with TV was on the left side (Fig. 1a, b). Such findings have also been observed with a Ga-68-labeled PSMA agent using an isocontour threshold of 50 % [13]. Notably, the correlation coefficients were rather low in the previous investigation, and this was similar to the herein obtained ρ values [13]. Nonetheless, in the present study, the sink effect was not observed across all of the studied organs. Thus, given the minimal impact of uptake on normal organs in patients with higher tumor burden, other factors may play a more crucial role in dosimetry with $[^{18}F]DCFPyL$. In a further analysis of our research group investigating the inter-patient and intra-patient variability of semiquantitative parameters in the most relevant normal organs, significant variability in $[^{18}F]DCFPyL$ uptake was noted [14]: over

Table 2. Descriptive statistics of normal organs and tumor burden

Compartment	Parameter	Minimum	Median	Maximum	Mean ^a	StDev ^a
Lacrimal gland L	SUL_{mean}	1.8	3.6	5.2	3.7	0.7
	SUV_{mean}	2.4	4.9	6.7	5	0.9
Lacrimal gland R	SUL_{mean}	2.4	3.7	5.6	3.7	0.7
	SUV_{mean}	3.3	5.1	7	5.1	0.9
Parotid gland L	SUL_{mean}	3	6	11.1	6.2	1.9
	SUV_{mean}	5	8.1	13.8	8.3	2.4
Parotid gland R	SUL_{mean}	2	6.3	11.3	6.3	1.9
	SUV_{mean}	4.9	8.2	14.2	8.5	2.4
SMG L	SUL_{mean}	3.3	5.8	13.5		
	SUV_{mean}	5	7.9	17.5		
SMG R	SUL_{mean}	1.9	5.9	13.1		
	SUV_{mean}	4	8	16.8		
Liver	SUL_{mean}	2.6	3.7	4.7	3.7	0.5
	SUV_{mean}	3.5	5	6.3	5	0.7
Spleen	SUL_{mean}	0.8	2.6	7.8		
	SUV_{mean}	1.3	3.7	14.4		
Kidney L	SUL_{mean}	7.8	16.6	28.7	17.4	5
	SUV_{mean}	10.5	22.8	41.3		
Kidney R	SUL_{mean}	11.4	17.3	30.9	18.1	5
	SUV_{mean}	11.2	23.4	43.6		
Tumor burden	SUL_{mean}	1.3	3.9	42.9		
	SUL_{max}	1.7	5.3	55.6		
	SUV_{mean}	1.6	5.4	57.9		
	TV	0.3	4.8	98.4		
	FTA	1.0	25.9	1752		

SUL_{mean} mean standardized uptake value corrected to lean body mass, SUV_{mean} mean standardized uptake value corrected to body weight, SMG submandibular gland, SUL_{max} the maximum standardized uptake value corrected to lean body mass, TV tumor volume (in ml), FTA fractional tumor activity in the volume of interest, L left, R right

^aMean and standard deviation (StDev) are not shown when the Shapiro-Wilk test excluded a normal distribution

Table 3. Correlation between organ-derived values and tumor burden based on [¹⁸F]DCFPyL PET. Spearman's rho (ρ), and the two-sided significance p is shown. The following tumor burden parameters are displayed: SUV_{mean} mean standardized uptake value corrected to body weight, $SUL_{mean/max}$ mean/maximum standardized uptake value corrected to lean body mass, TV tumor volume, FTA fractional tumor activity in the volume of interest. Submandibular glands (SMGs). * $p < 0.05$

Tumor burden-derived parameters			SUV_{mean}	SUL_{mean}	SUL_{max}	TV	FTA
Kidney L	SUV_{mean}	ρ	-0.152	-0.161	-0.22	-0.214	-0.226
		p	0.54	0.46	0.41	0.049*	0.160
	SUL_{mean}	ρ	-0.232	-0.24	-0.282	-0.176	-0.255
		p	0.14	0.12	0.09	0.041*	0.112
Kidney R	SUV_{mean}	ρ	-0.147	-0.167	-0.204	-0.137	-0.160
		p	0.64	0.3	0.52	0.06	0.325
	SUL_{mean}	ρ	-0.23	-0.25	-0.28	-0.165	-0.245
		p	0.18	0.14	0.12	0.05	0.127
Parotid L	SUV_{mean}	ρ	-0.129	-0.088	-0.081	0.148	0.012
		p	0.39	0.55	0.67	0.79	0.944
	SUL_{mean}	ρ	-0.154	-0.117	-0.103	0.148	-0.002
		p	0.26	0.37	0.45	0.4	0.992
Parotid R	SUV_{mean}	ρ	-0.188	-0.155	-0.168	0.167	-0.010
		p	0.29	0.37	0.37	0.71	0.952
	SUL_{mean}	ρ	-0.188	-0.155	-0.168	0.125	-0.046
		p	0.2	0.36	0.26	0.4	0.779
Lacrimal gland L	SUV_{mean}	ρ	-0.038	-0.008	-0.012	0.041	0.037
		p	0.81	0.96	0.94	0.8	0.823
	SUL_{mean}	ρ	-0.099	-0.078	-0.064	0.069	-0.018
		p	0.54	0.63	0.7	0.67	0.912
Lacrimal gland R	SUV_{mean}	ρ	0.044	0.053	0.083	0.044	-0.005
		p	0.78	0.74	0.61	0.79	0.974
	SUL_{mean}	ρ	-0.037	0.003	-0.021	0.05	-0.061
		p	0.82	0.99	0.9	0.76	0.708
SMG L	SUV_{mean}	ρ	-0.311	-0.28	-0.263	0.292	0.014
		p	0.05	0.08	0.1	0.067	0.933
	SUL_{mean}	ρ	-0.269	-0.255	-0.237	0.246	-0.004
		p	0.09	0.11	0.14	0.13	0.982
SMG R	SUV_{mean}	ρ	-0.238	-0.213	-0.215	0.352	0.108
		p	0.14	0.19	0.18	0.03	0.509
	SUL_{mean}	ρ	-0.247	-0.232	-0.231	0.287	0.044
		p	0.12	0.15	0.15	0.07	0.789
Spleen	SUV_{mean}	ρ	-0.214	-0.171	-0.244	0.005	-0.199
		p	0.283	0.582	0.523	0.99	0.219
	SUL_{mean}	ρ	-0.23	0.18	-0.25	-0.028	-0.234
		p	0.14	0.31	0.26	0.96	0.146
Liver	SUV_{mean}	ρ	0.005	0.001	-0.037	-0.172	-0.136
		p	0.9	0.9	0.8	0.3	0.402
	SUL_{mean}	ρ	-0.119	-0.114	-0.154	-0.15	-0.243
		p	0.29	0.31	0.23	0.47	0.132

time, the liver and kidneys showed the greatest degree of variability for intra-patient factors (*e.g.*, time of day, recent meals, hydration status, and therapies during the time interval between subsequent [¹⁸F]DCFPyL scans). This was in contradistinction to the variability in normal lacrimal glands, salivary glands, and spleen, which primarily depend upon inter-patient factors (*e.g.*, weight, height, body composition, and differences in prior therapies) [15]. Thus, integrating the available information of our two studies investigating semiquantitative parameters with [¹⁸F]DCFPyL, the inter-/intra-patient variability would be a much more important consideration for personalized dosimetry with PSMA-targeted therapeutic agents structurally related to [¹⁸F]DCFPyL than the tumor burden.

In light of the present study showing no tumor sink effect with [¹⁸F]DCFPyL, a peritherapeutic dosimetry for RLT planning may serve as an attractive alternative for a more

reliable dose estimate. Albeit such a procedure may be challenging for both patients and personnel [24, 25], it may be considered for every individual to safely determine the appropriate amount of activity to be administered in a therapeutic setting [26]. Extrapolation of the results of this study to therapeutic radionuclides that are structurally similar to [¹⁸F]DCFPyL but still vary in aspects of their chemical structures must be made with caution, although the similar biodistributions of many PSMA-targeted agents suggests that these findings may still be directly relevant.

The present study has several limitations: First, a larger assessment with more patients is warranted to confirm our preliminary findings. However, on an intra-tumor parameter level, highly significant correlations were achieved, which may serve as quality control metrics for the present study (data not shown). Apart from that, one may speculate if a more sustainable tumor sink effect (*e.g.*, in the kidneys) may

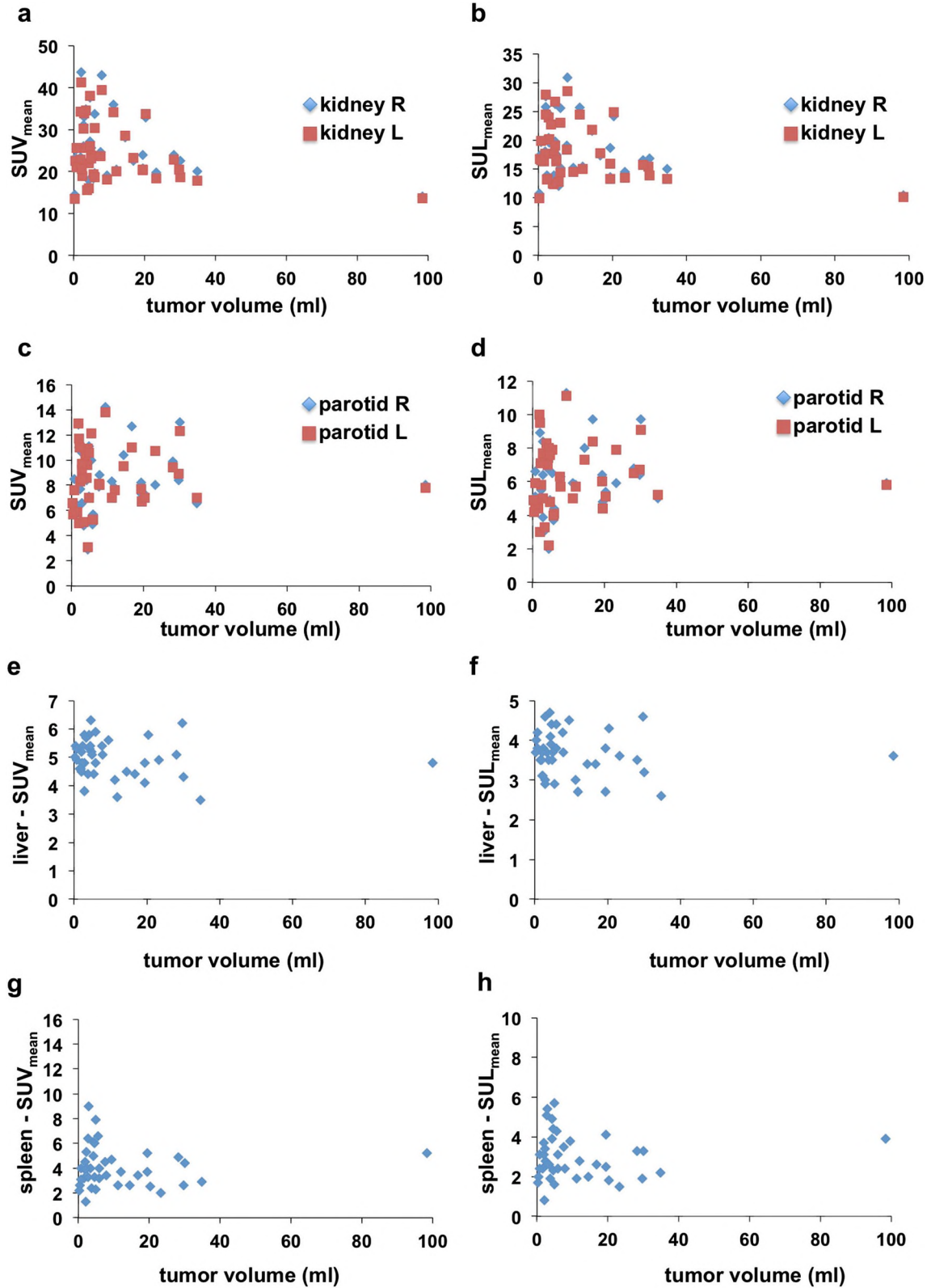


Fig. 1. Correlative plots of uptake in selected normal organs with [¹⁸F]DCFPyL-derived tumor volume (intensity threshold, 50 %). The **a** SUV_{mean} and **b** SUL_{mean} of the left kidney (red) correlated significantly with tumor volume ($p < 0.05$). **a** SUV_{mean} and **b** SUL_{mean} of the left (L) and right (R) kidneys, **c** SUV_{mean} and **d** SUL_{mean} of the left and right parotid glands, **e** SUV_{mean} and **f** SUL_{mean} of the liver, **g** SUV_{mean} and **h** SUL_{mean} of the spleen. SUV_{mean} = mean standardized uptake value corrected to body weight, SUL_{max} = the maximum standardized uptake value corrected to lean body mass.

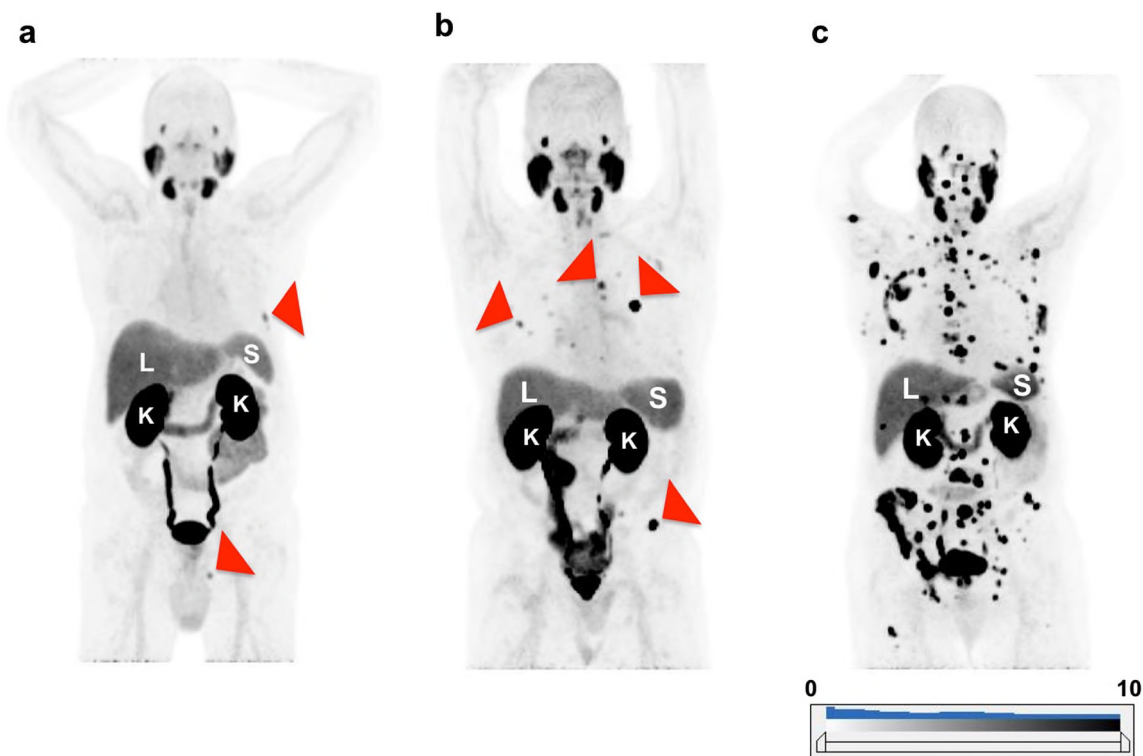


Fig. 2. [^{18}F]DCFPyL maximum intensity projection (MIP) of patients with **a** low, **b** intermediate, and **c** high tumor burden. Spleen (S), liver (L), and kidneys (K) are indicated. Red arrows indicate representative tumor lesions, which can be detected on the MIPs: In patient **a**: metastases in the seventh rib (left) and in the left ischium are indicated. In patient **b**: multiple bone lesions are indicated. Patient **c** shows a near-superscan with extensive involvement in the skeleton. The uptake in normal organs (visible for liver, kidneys, and spleen) does not differ visually among the different patients.

be achieved if more patients with higher tumor burden are included [13]. However, the current *post hoc* analysis also investigated such superscans (*e.g.*, with extensive skeletal involvement; Fig. 2c) and the randomly selected cases may rather reflect a more “real-world” scenario, as no preselection of patients with different amounts of tumor burden was conducted. Nonetheless, the herein derived results even in patients with rather low tumor burden may be of utmost importance, as PSMA-PET is more routinely used in patients with low or even ultra-low PSA levels [27].

Conclusion

In the present analysis with the PSMA-targeted radiotracer [^{18}F]DCFPyL, only a modest tumor sink effect was observed for selected uptake parameters for the kidneys whereas for most normal organs, no sink effect was seen. While statistically significant, the effect in the kidneys is very small (ρ , range, -0.176 to -0.214) and unlikely to be clinically relevant. Thus, other factors, such as the relatively high intra-patient variability for normal organ uptake described in our companion paper, may be a much more important considerations for personalized dosimetry with PSMA-targeted therapeutic agents structurally related to [^{18}F]DCFPyL.

Sources of Funding. Progenics Pharmaceuticals, The Prostate Cancer Foundation Young Investigator Award, and National Institutes of Health grants CA134675, CA183031, CA184228, and EB024495.

Compliance with Ethical Standards

Conflict of Interest

Martin G. Pomper is a coinventor on a patent covering [^{18}F]DCFPyL and is entitled to a portion of any licensing fees and royalties generated by this technology. This arrangement has been reviewed and approved by the Johns Hopkins University in accordance with its conflict-of-interest policies. He has also received research funding from Progenics Pharmaceuticals, the licensee of [^{18}F]DCFPyL. Michael A. Gorin has served as a consultant to, and has received research funding from, Progenics Pharmaceuticals. Kenneth J. Pienta has received research funding from Progenics Pharmaceuticals. Steven P. Rowe has received research funding from Progenics Pharmaceuticals.

References

1. Gorin MA, Pomper MG, Rowe SP (2016) PSMA-targeted imaging of prostate cancer: the best is yet to come. *BJU Int* 117:715–716
2. Sheikhabaei S, Afshar-Oromieh A, Eiber M, Solnes LB, Javadi MS, Ross AE, Pienta KJ, Allaf ME, Haberkorn U, Pomper MG, Gorin MA, Rowe SP (2017) Pearls and pitfalls in clinical interpretation of prostate-specific membrane antigen (PSMA)-targeted PET imaging. *Eur J Nucl Med Mol Imaging* 44:2117–2136
3. Eiber M, Herrmann K, Fendler WP, Maurer T (2016) ^{68}Ga -labeled prostate-specific membrane antigen positron emission tomography for

- prostate cancer imaging: the new kid on the block—early or too early to draw conclusions? *Eur Urol* 70:938–940
4. Kesch C, Kratochwil C, Mier W, Kopka K, Giesel FL (2017) ^{68}Ga or ^{18}F for prostate cancer imaging? *J Nucl Med* 58:687–688
 5. Szabo Z, Mena E, Rowe SP, Plyku D, Nidal R, Eisenberger MA, Antonarakis ES, Fan H, Dannals RF, Chen Y, Mease RC, Vranesic M, Bhatnagar A, Sgouros G, Cho SY, Pomper MG (2015) Initial evaluation of [^{18}F]DCFPyL for prostate-specific membrane antigen (PSMA)-targeted PET imaging of prostate cancer. *Mol Imaging Biol* 17:565–574
 6. Dietlein M, Kobe C, Kuhnert G, Stockter S, Fischer T, Schomäcker K, Schmidt M, Dietlein F, Zlatopolskiy BD, Krapf P, Richarz R, Neubauer S, Drzezga A, Neumaier B (2015) Comparison of [^{18}F]DCFPyL and [^{68}Ga]Ga-PSMA-HBED-CC for PSMA-PET imaging in patients with relapsed prostate cancer. *Mol Imaging Biol* 17:575–584
 7. Werner RA, Andree C, Javadi MS, Lapa C, Buck AK, Higuchi T, Pomper MG, Gorin MA, Rowe SP, Pienta KJ (2018) A voice from the past: rediscovering the virchow node with prostate-specific membrane antigen-targeted ^{18}F -DCFPyL positron emission tomography imaging. *Urology* 117:18–21
 8. Werner RA, Weich A, Kircher M, Solnes LB, Javadi MS, Higuchi T, Buck AK, Pomper MG, Rowe SP, Lapa C (2018) The theranostic promise for neuroendocrine tumors in the late 2010s - where do we stand, where do we go? *Theranostics* 8:6088–6100
 9. Prasad V, Baum RP (2010) Biodistribution of the Ga-68 labeled somatostatin analogue DOTA-NOC in patients with neuroendocrine tumors: characterization of uptake in normal organs and tumor lesions. *Q J Nucl Med Mol Imaging* 54:61–67
 10. Liu Y (2011) Super-superscan on a bone scintigraphy. *Clin Nucl Med* 36:227–228
 11. Beauregard JM, Hofman MS, Kong G, Hicks RJ (2012) The tumour sink effect on the biodistribution of ^{68}Ga -DOTA-octreotate: implications for peptide receptor radionuclide therapy. *Eur J Nucl Med Mol Imaging* 39:50–56
 12. Werner RA, Hanscheid H, Leal JP et al (2018) Impact of tumor burden on quantitative [^{68}Ga] DOTATATE biodistribution. *Mol Imaging Biol*. In Press.
 13. Gaertner FC, Halabi K, Ahmadzadehfar H, Kürpig S, Eppard E, Kotsikopoulos C, Liakos N, Bundschuh RA, Strunk H, Essler M (2017) Uptake of PSMA-ligands in normal tissues is dependent on tumor load in patients with prostate cancer. *Oncotarget* 8:55094–55103
 14. Sahakyan K, Li X, Lodge MA, et al. (2019) Semiquantitative parameters in PSMA-targeted PET imaging with ^{18}F -DCFPyL: inpatient and interpatient variability of normal organ uptake. *Mol Imaging Biol*. In Press.
 15. Werner RA, Bundschuh RA, Bundschuh L, Javadi MS, Leal JP, Higuchi T, Pienta KJ, Buck AK, Pomper MG, Gorin MA, Lapa C, Rowe SP (2018) Interobserver agreement for the standardized reporting system PSMA-RADS 1.0 on ^{18}F -DCFPyL PET/CT imaging. *J Nucl Med* 59:1857–1864
 16. Ravert HT, Holt DP, Chen Y, Mease RC, Fan H, Pomper MG, Dannals RF (2016) An improved synthesis of the radiolabeled prostate-specific membrane antigen inhibitor, [^{18}F]DCFPyL. *J Label Comp Radiopharm* 59:439–450
 17. Werner RA, Sheikhabaei S, Jones KM, Javadi MS, Solnes LB, Ross AE, Allaf ME, Pienta KJ, Lapa C, Buck AK, Higuchi T, Pomper MG, Gorin MA, Rowe SP (2017) Patterns of uptake of prostate-specific membrane antigen (PSMA)-targeted ^{18}F -DCFPyL in peripheral ganglia. *Ann Nucl Med* 31:696–702
 18. Rowe SP, Pienta KJ, Pomper MG, Gorin MA (2018) PSMA-RADS version 1.0: a step towards standardizing the interpretation and reporting of PSMA-targeted PET imaging studies. *Eur Urol* 73:485–487
 19. Rowe SP, Pienta KJ, Pomper MG, Gorin MA (2018) Proposal for a structured reporting system for prostate-specific membrane antigen-targeted PET imaging: PSMA-RADS version 1.0. *J Nucl Med* 59:479–485
 20. Li X, Rowe SP, Leal JP, Gorin MA, Allaf ME, Ross AE, Pienta KJ, Lodge MA, Pomper MG (2017) Semiquantitative parameters in PSMA-targeted PET imaging with (18)F-DCFPyL: variability in normal-organ uptake. *J Nucl Med* 58:942–946
 21. Schmidkonz C, Cordes M, Schmidt D, Bäuerle T, Goetz TI, Beck M, Prante O, Cavallaro A, Uder M, Wullich B, Goebell P, Kuwert T, Ritt P (2018) ^{68}Ga -PSMA-11 PET/CT-derived metabolic parameters for determination of whole-body tumor burden and treatment response in prostate cancer. *Eur J Nucl Med Mol Imaging* 45:1862–1872
 22. Schmuck S, von Klot CA, Henkenberens C, Sohns JM, Christiansen H, Wester HJ, Ross TL, Bengel FM, Derlin T (2017) Initial experience with volumetric ^{68}Ga -PSMA I&T PET/CT for assessment of whole-body tumor burden as a quantitative imaging biomarker in patients with prostate cancer. *J Nucl Med* 58:1962–1968
 23. Rowe SP, Macura KJ, Mena E, Blackford AL, Nadal R, Antonarakis ES, Eisenberger M, Carducci M, Fan H, Dannals RF, Chen Y, Mease RC, Szabo Z, Pomper MG, Cho SY (2016) PSMA-based [^{18}F]DCFPyL PET/CT is superior to conventional imaging for lesion detection in patients with metastatic prostate cancer. *Mol Imaging Biol* 18:411–419
 24. Hanscheid H, Lapa C, Buck AK, Lassmann M, Werner RA (2018) Dose mapping after endoradiotherapy with ^{177}Lu -DOTATATE/DOTATOC by a single measurement after 4 days. *J Nucl Med* 59:75–81
 25. Hanscheid H, Lapa C, Buck AK, Lassmann M, Werner RA (2017) Absorbed dose estimates from a single measurement one to three days after the administration of ^{177}Lu -DOTATATE/-TOC. *Nuklearmedizin* 56:219–224
 26. Eberlein U, Cremonesi M, Lassmann M (2017) Individualized dosimetry for theranostics: necessary, nice to have, or counterproductive? *J Nucl Med* 58:97S–103S
 27. Giesel FL, Knorr K, Spohn F, Will L, Maurer T, Flechsig P, Neels O, Schiller K, Amaral H, Weber WA, Haberkorn U, Schwaiger M, Kratochwil C, Choyke P, Kramer V, Kopka K, Eiber M (2019) Detection efficacy of ^{18}F -PSMA-1007 PET/CT in 251 patients with biochemical recurrence of prostate cancer after radical prostatectomy. *J Nucl Med* 60:362–368